Science Press

Trans. Nonferrous Met. Soc. China 17(2007) s978−s984

Transactions of Nonferrous Metals Society of China

www.csu.edu.cn/ysxb/

# Low-temperature performance and high-rate discharge capability of $AB_5$-type non-stoichiometric hydrogen storage alloy

LU Yan-jing(陆延静), ZHU Lei(朱 磊), CHENG Yan(成 艳),
CHEN Hui(陈 晖), JIAN Xu-yu(简旭宇), WANG Zhong(王 忠)

Energy Material and Technology Research Institute, General Research Institute for Nonferrous Metals, Beijing 100088, China

Received 15 July 2007; accepted 10 September 2007

**Abstract:** Low-temperature performance and high-rate discharge capability of $AB_5$-type non-stoichiometric hydrogen storage are studied. X-ray diffraction(XRD), pressure-composition-temperature(PCT) curves and electrochemical impedance spectroscopy(EIS) are applied to characterize the electrochemical properties of $AB_x$ ($x$=4.8, 4.9, 5.0, 5.1, 5.2) alloys. The results show that the non-stoichiometric alloys exhibit better electrochemical properties compared with that of the $AB_5$ alloy.

**Key words:** $AB_5$-type hydrogen storage alloy; non-stoichiometry; low-temperature performance; high-rate discharge capability

## 1 Introduction

In recent years, nickel-metal hydride(Ni-MH) secondary batteries have been widely used in various portable electronic devices, electric tools and vehicles because of their excellent electrochemical performance and environmental compatibility[1]. However, the low-temperature performance of Ni-MH batteries is unsatisfied. As we known, hydrogen storage alloys play a key role in the discharging process at low temperature for Ni-MH battery. At present, the commercialized negative electrode materials are mainly $AB_5$-type alloys due to its long-term cycling stability, high-rate capacity, and good charge-discharge kinetics[2−5]. Therefore, it is necessary to improve the low-temperature electro-chemical performances of hydrogen storage alloy.

To our knowledge, no systematically investigation has been done for the $AB_5$-type non-stoichiometric alloys under high rate and low temperature. In this work, the performance of the $AB_5$-type non-stoichiometric alloys are investigated.

## 2 Experimental

Based upon the $AB_5$-type $(LaCePr)(NiCoMnAl)_5$ hydrogen alloy, $(LaCePr)(NiCoMnAl)_x$ ($x$=4.8, 4.9, 5.0, 5.1, 5.2) non-stoichiometric alloys were designed and prepared by induction melting under argon shield of pure elements in a water-cooled copper crucible. The ingots were melted and turned over three times for homogeneity Then the ingots were crushed and mechanically grounded to a particle size of less than 74 μm.

The crystal structures of $(LaCePr)(NiCoMnAl)_x$ (replaced by $AB_x$ in the following) were analyzed by X-ray diffractogram.

### 2.1 Preparation of the MH electrode

0.1 g alloy powder was mixed uniformly with 0.3 g nickel powder in proportion of 1:3, and then they were pressed by 20 MPa into the negative plate 13 mm in diameter and 0.5 mm in thickness. The counter electrode was formed by the $NiOOH/Ni(OH)_2$, whereas the reference electrode was Hg/HgO electrode filled with 6 mol/L KOH solution.

### 2.2 Electrochemical measurements

After activation at room temperature (20 ℃), the electrodes were charged for 7 h at 60 mA/g (0.2C), then some were kept for 30 min at room temperature and the others were placed in the low temperature cabinets for 4 h and 6 h at the temperature of −20 ℃ and −40 ℃,

**Foundation item:** Project(2006AA11A151) supported by the National Hi-Tech Research and Development Program of China
**Corresponding author:** LU Yan-jing; Tel: +86-10-82241241; E-mail: luyanjing82@126.com

respectively, then the samples were discharged at various rates (0.2*C*, 0.5*C*, 1*C* and 3*C*) to −0.6, −0.6, −0.5, −0.4 voltage with respect to Hg/HgO reference electrode.

Pressure-composition-temperature(PCT) curves of the alloys were determined by electrochemical methods[6]. The thermodynamics parameters including the equilibrium pressure of the hydrogen absorption or desorption and the change of enthalpy were calculated.

The electrochemical impedance spectroscopies of the 50%DOD (depth of discharge) electrodes were measured and the scan frequency was from 100 kHz to 1 mHz.

## 3 Results and discussion

### 3.1 Discharge capacity of electrode

Fig.1 shows the variation of the discharge capacity, versus the value of *x* of the AB*x* alloy. It can be seen that with the increase of *x*, the discharge capacities curves of various rates (0.2*C*, 0.5*C*, 1*C*, 3*C*) at 20 ℃ and −20 ℃, as well as that of 0.2*C* at −40 ℃, present the shape of character M. Over-stoichiometric alloys and under-stoichiometric alloys exhibit better high-rate discharge capability and low-temperature performance compared with that of the stoichiometric alloy (*x*=5.0). The alloy with *x*=5.1 shows the excellent electrochemical capability, of which the 3*C* discharge capacity reaches 284 mA·h/g at 20 ℃, and 0.2*C* also reaches 233 mA·h/g at −40 ℃.

### 3.2. Structural analysis

The XRD patterns of $AB_x$ metal-hydride alloys are given in Fig.2. The results show that all alloys keep the typical single phase of $CaCu_5$.The lattice parameters and lattice volume are calculated and compiled in Table 1. It can be seen that with the increase of the value of *x*, The lattice parameters *c* first increase and then decrease, which is similar to the behaviour of the low-temperature discharge capacity. On the contrary, the lattice parameters *a* exhibit the opposite phenomenon. The variation of lattice parameters and volume as a function of *x* is showed in Fig.3. The alloys with smaller lattice parameter *a* and larger lattice parameter *c* show better low-temperature performances and high-rate discharge capabilities.

**Table 1** Smaller (a) and bigger (b) lattice parameters and lattice volume(*V*) of $AB_x$ metal- hydride alloys

| Compound | *a*/nm | *c*/nm | *V*/nm$^3$ |
|---|---|---|---|
| $AB_{4.8}$ | 0.499 5 | 0.404 6 | 0.087 43 |
| $AB_{4.9}$ | 0.499 3 | 0.405 8 | 0.087 60 |
| $AB_{5.0}$ | 0.502 6 | 0.415 2 | 0.087 83 |
| $AB_{5.1}$ | 0.499 9 | 0.403 9 | 0.087 40 |
| $AB_{5.2}$ | 0.500 0 | 0.402 3 | 0.087 10 |

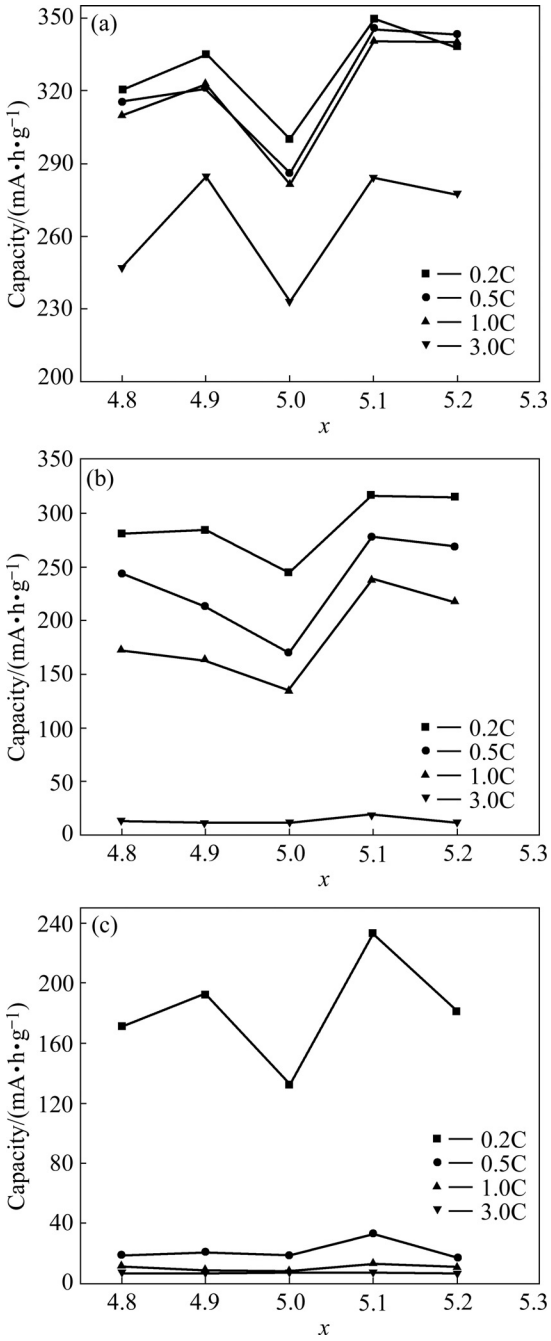


**Fig.1** Variation of different rate discharge capacities with *x* for $AB_x$ alloys at different temperatures: (a) 20 ℃; (b) −20 ℃; (c) −40 ℃

### 3.3 Thermodynamic properties

The pressure-composition-temperature(P—C—T) curves measured at 20, −20 and −40 ℃ are shown in Fig.4.

The equilibrium pressure of hydrogen absorption or desorption ($P_{eq}$) are defined as following equation[7]:

$$P_{eq} = \frac{P_2 + P_1}{2} \quad (1)$$

where $P_2$ and $P_1$ are the pressures of inflection points of curves in Fig.4. The variation of $P_{eq}$ versus the value

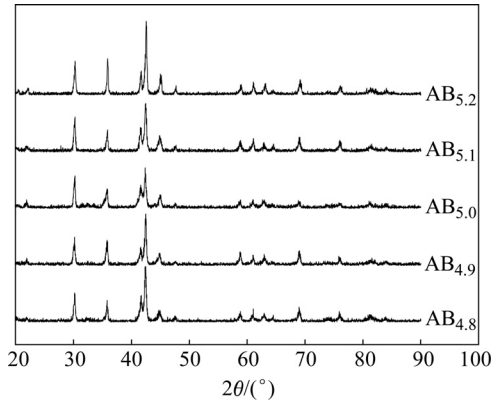


**Fig.2** XRD patterns of of $AB_x$ metal-hydride alloys

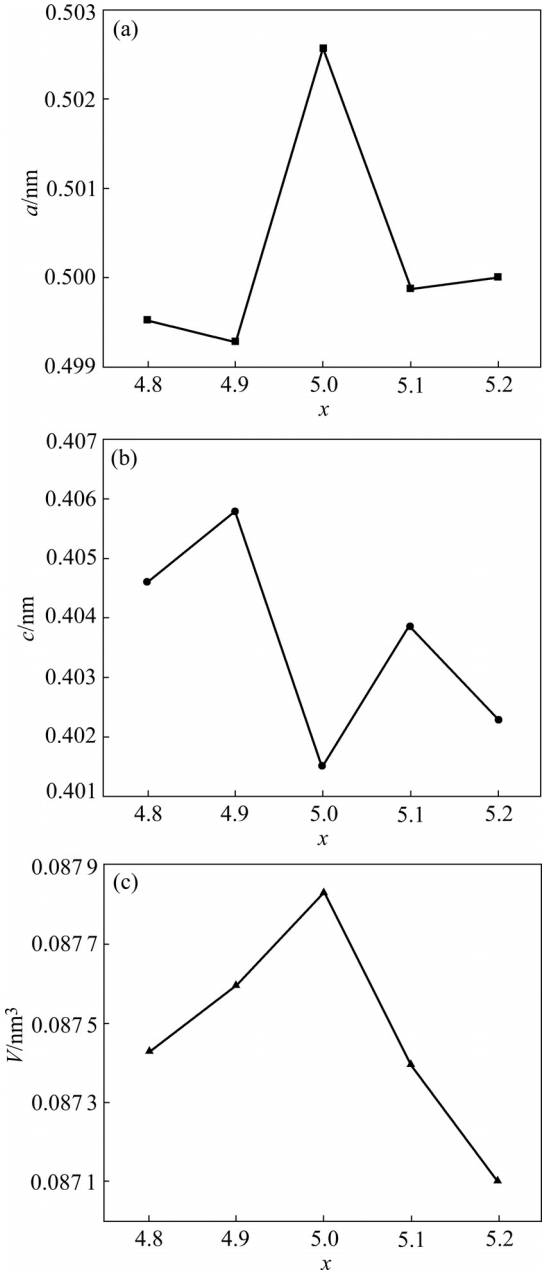


**Fig.3** Variation of lattice parameters (*a*, *c*) and lattice volume (*V*) of $AB_x$ metal-hydride alloys as function of *x*: (a) *a*; (b) *c*; (c) *V*

of *x* is given in Fig.5. According to $P_{eq}$, Van't Hoff curves of $AB_x$ alloys is presented in Fig.6, and the variation of the change of enthalpy($\Delta H$) of $AB_x$ alloys as a function of *x* is given in Fig.7.

The results show that over-stoichiometric alloys and under-stoichiometric alloys present higher equilibrium pressure ($P_{eq}$) and less absolute value of the change of enthalpy ($|\Delta H|$). The alloy with $x$=5.0 exhibit the lowest $P_{eq}$ and the highest $|\Delta H|$, while the alloy with $x$=5.1 shows the higher $P_{eq}$ and the least $|\Delta H|$, and its $|\Delta H|$ reaches 28.9 kJ/mol. With the increase of the value of *x*, the change of enthalpy ($\Delta H$) shows the same tendency as that of the discharge capacities, which indicates that there is a close relationship between the electrochemical property and the thermodynamic performance for non-stoichiometric alloys. The alloys with higher equilibrium pressure and less absolute value of enthalpy display higher high-rate discharge capacities and low-temperature capabilities, which may be ascribed to the poor stability of metal hydrides materials.

### 3.4 Electrochemical impedance spectroscopy

Electrochemical impedance is a powerful tool for characterization of metal-hydride electrodes, and has been widely used[8−10]. According to the mathematical model developed by WANG et al[11], the charge-transfer resistance, $R_t$, could be calculated from the electrochemical impedance spectroscopy(EIS) by constructing the equivalent circuit, and the exchange current density ($I_0$) could be defined as following equation[12]:

$$I_0 = \frac{RT}{mFR_t} \tag{2}$$

where $R$, $T$, $m$ and $F$ are the gas constant, the absolute temperature, the effective mass of material and the Faraday constant, respectively.

Fig.8 shows the Nyquist plot of $AB_x$ metal-hydride alloys with 50%DOD, and the calculated $R_t$ and $I_0$ are listed in Table 2 and Table 3.

Fig.9 shows the variation of the exchange current density ($I_0$) of $AB_x$ metal-hydride alloys (50%DOD) as a function of *x*. With the increase of *x*, the exchange current densities of $AB_x$ alloys present the same tendency as that of the discharge capacities, and the exchange current densities of the non-stoichiometric alloys are higher than that of $AB_5$ alloy. The high-rate discharge capacities increase gradually with the increase of the exchange current density[13−15]. It is well known that the high exchange current density indicates not only the high reaction rate of the electrode, i.e. high rate charge-discharge capability, but also a low degradation rate of electrode performance[16]. Thus, we can conclude that the non-stoichiometry is beneficial to the

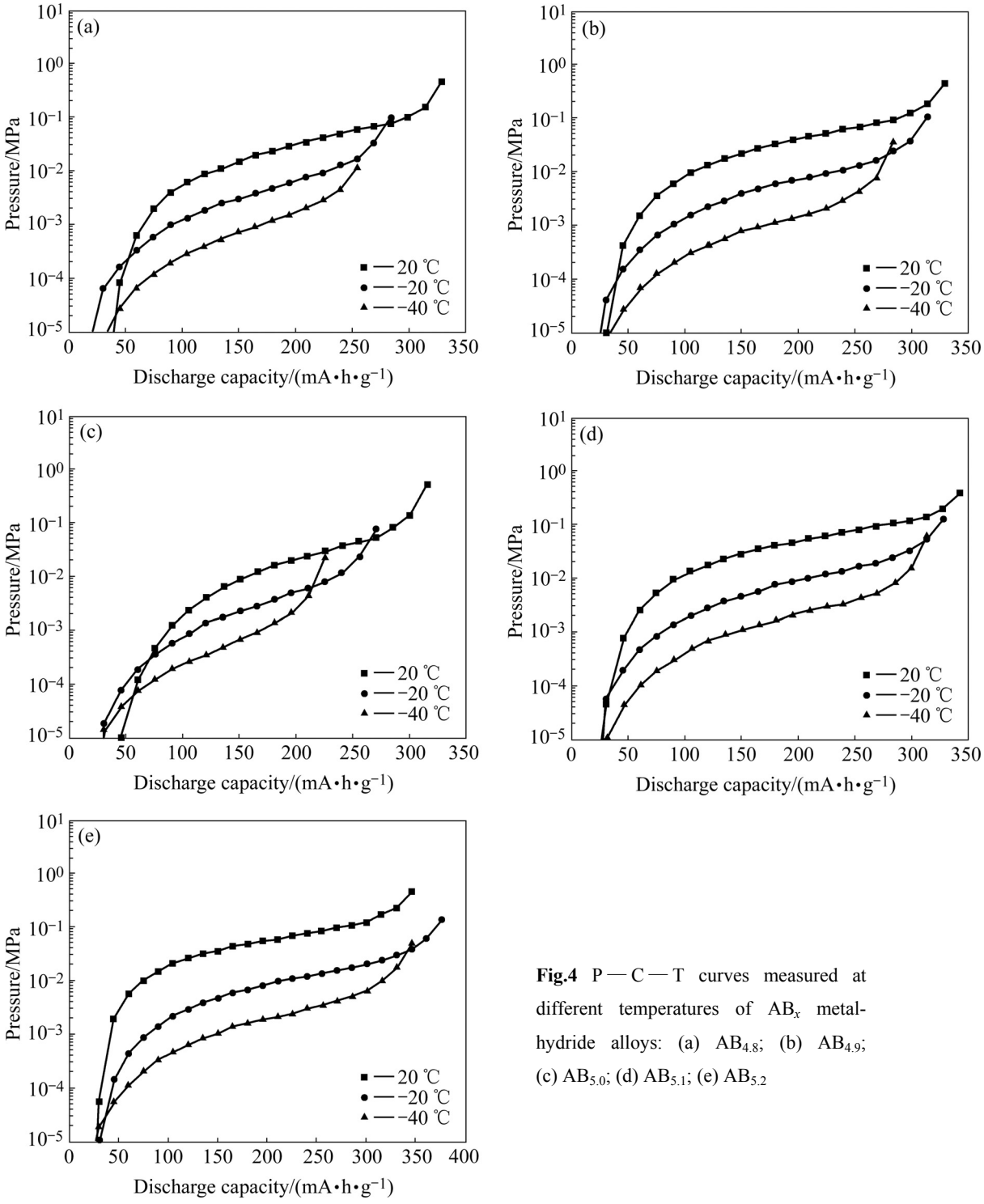


**Fig.4** P — C — T curves measured at different temperatures of $AB_x$ metal-hydride alloys: (a) $AB_{4.8}$; (b) $AB_{4.9}$; (c) $AB_{5.0}$; (d) $AB_{5.1}$; (e) $AB_{5.2}$

**Table 2** Charge-transfer resistance ($R_t$) of $AB_x$ metal-hydride alloys (50%DOD) at different temperatures

| $T$/K | $R_t$/ Ω | | | | |
|---|---|---|---|---|---|
| | $AB_{4.8}$ | $AB_{4.9}$ | $AB_{5.0}$ | $AB_{5.1}$ | $AB_{5.2}$ |
| 293 | 0.276 6 | 0.246 6 | 0.405 4 | 0.267 9 | 0.477 9 |
| 253 | 3.531 0 | 3.332 0 | 7.944 0 | 2.966 0 | 5.067 0 |
| 233 | 16.810 0 | 13.100 0 | 41.440 0 | 11.670 0 | 21.520 0 |

**Table 3** Exchange current density ($I_0$) of $AB_x$ metal-hydride alloys (50%DOD) at different temperatures

| $T$/K | $I_0$/(mA·g) | | | | |
|---|---|---|---|---|---|
| | $AB_{4.8}$ | $AB_{4.9}$ | $AB_{5.0}$ | $AB_{5.1}$ | $AB_{5.2}$ |
| 293 | 913.2 | 1024.3 | 623.1 | 942.9 | 528.6 |
| 253 | 59.4 | 65.5 | 27.5 | 73.5 | 43.1 |
| 233 | 11.9 | 15.3 | 4.84 | 17.2 | 9.3 |

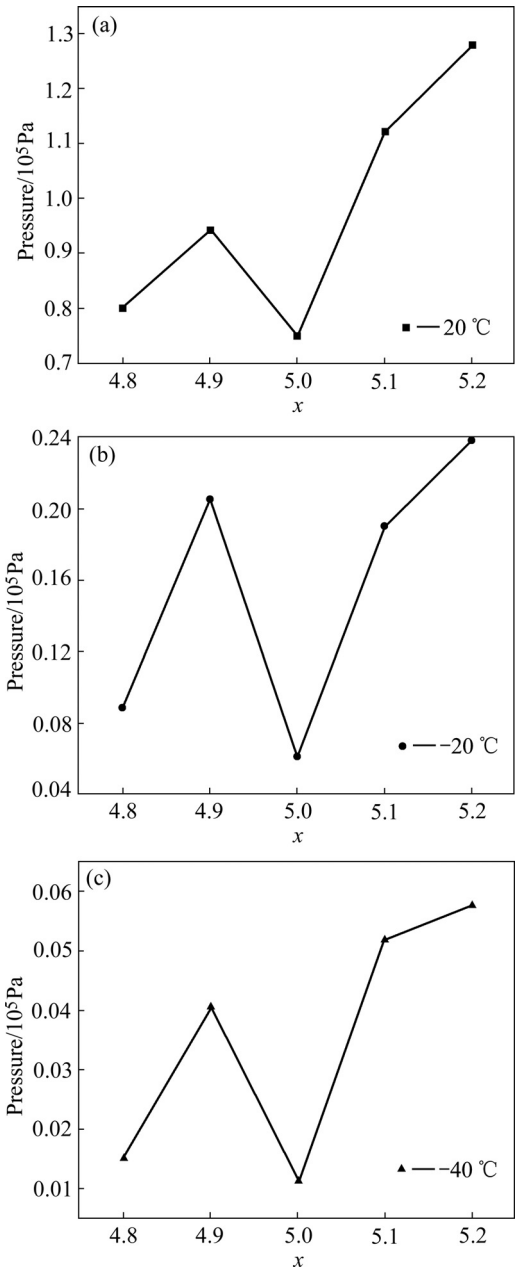


**Fig.5** Variation of equilibrium pressures of $AB_x$ metal-hydride alloys as function of $x$: (a) 20 ℃; (b) −20 ℃; (c) −40 ℃

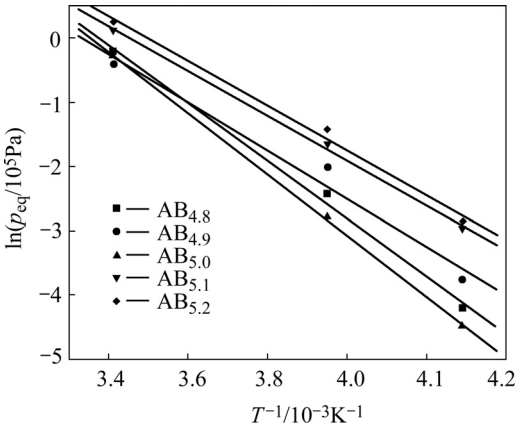


**Fig.6** Van't Hoff curves of $AB_x$ metal-hydride alloys

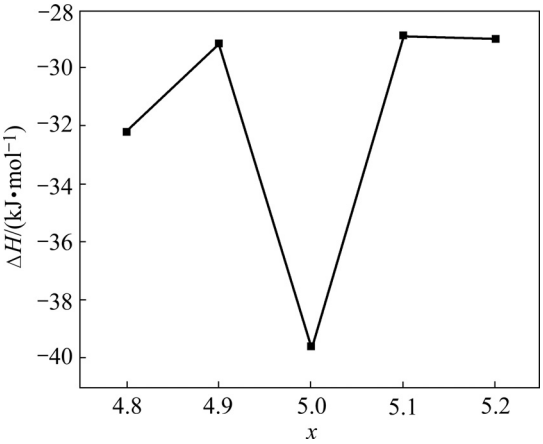


**Fig.7** Variation of enthalpy ($\Delta H$) of $AB_x$ metal-hydride alloys as function of $x$

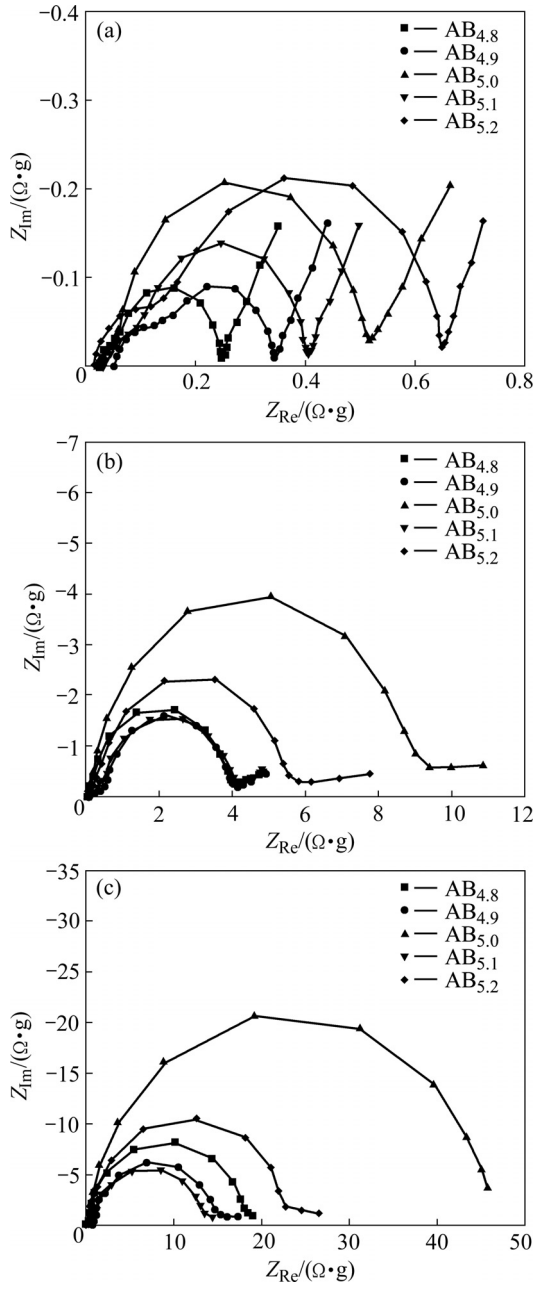


**Fig.8** Nyquist plots of $AB_x$ metal-hydride alloys (50%DOD)

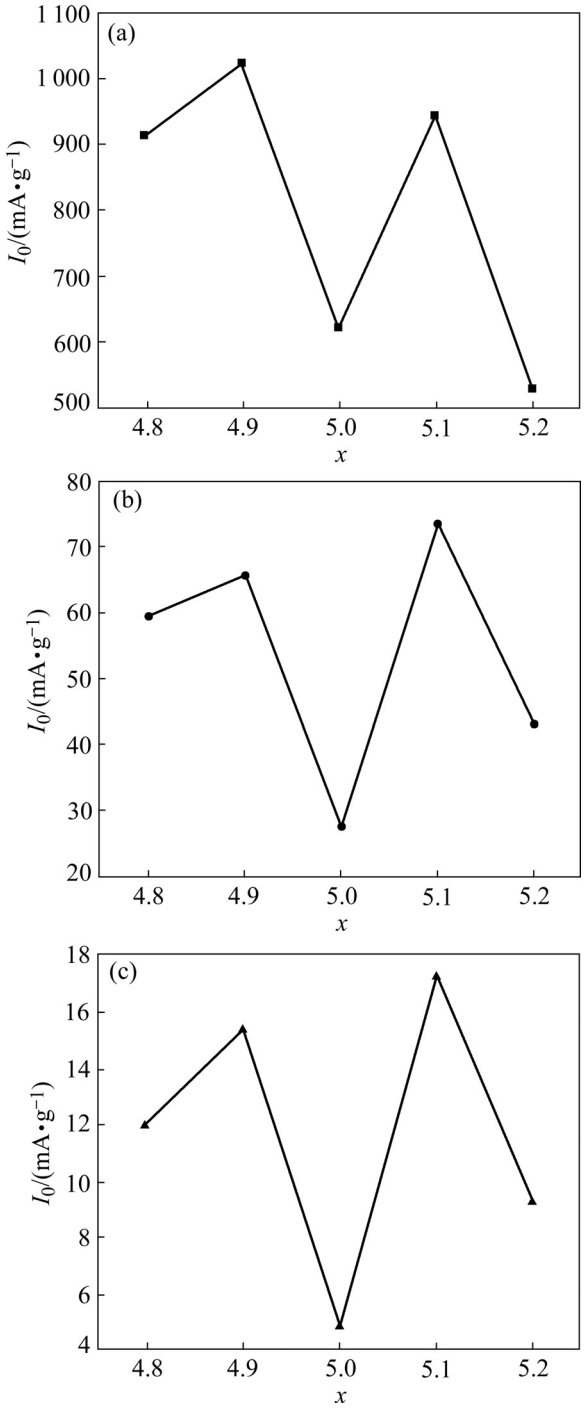


**Fig.9** Variation of exchange current density ($I_0$) of $AB_x$ metal-hydride alloys as function of $x$: (a) 20 ℃; (b) −20 ℃; (c) −40 ℃

increase of electrodes exchange current density, which can improve the low-temperature performance and high-rate discharge ability.

## 4 Conclusions

1) With the increase of $x$, the discharge capacities of $AB_x$ electrodes present the shape of "M". Under-stoichiometric and over-stoichiometric alloys present the better low-temperature performance and the higher high-rate discharge ability compared with that of the stoichiometric alloy ($x$=5.0).

2) Non-stoichiometric alloys possess smaller lattice parameter $a$ and bigger lattice parameter $c$, which may be beneficial to their low-temperature performance and high-rate discharge capability.

3) With the increase of $x$, the change of enthalpy ($\Delta H$) and the exchange current density ($I_0$) of $AB_x$ alloys show the same tendency as that of the discharge capacities, which indicate that there exists a close relationship between the $\Delta H$, $I_0$, low-temperature performance and high-rate discharge ability.

4) The $AB_{5.1}$ alloy, with the least $|\Delta H|$ and highest $I_0$, shows the best discharge capability. Its 3C discharge capacity reaches 284 mA·h/g at 20 ℃, while 0.2C reaches 233 mA·h/g at −40 ℃.

## References

[1] TLIHA M, KHALDI C, MATHLOUTHI H, LAMLOUMI J, PERCHERON-GUEGAN A. Electrochemical investigation of the iron-containing and no iron-containing AB5-type negative electrodes [J]. J Alloys Compd, 2007, 440(1/2): 323−327.

[2] RIVERA M A, PAL U, WANG Xian-you, GONZALEZ-RODRIGUEZ J G, GAMBOA S A. Rapid activation of $MmNi_{5-x}M_x$ based MH alloy through Pd nanoparticle impregnation [J]. J Power Sources, 2006, 155: 470−474.

[3] LI Rong, WU Jian-min, SU Hang, ZHOU Shao-xiong. Micro-structure and electrochemical performance of vanadium-containing $AB_5$-type low-Co intermetallic hydrides [J]. J Alloys Compd, 2006, 421: 258−267.

[4] YUAN Xian-xia, XU Nai-xin. Determination of hydrogen diffusion coefficient in metal hydride electrode by cyclic voltammetry [J]. J Alloys Compd, 2001, 316(1/2): 113−117.

[5] LI Shang, PAN Gui-ling, ZHANG Ying, GAO Xue-ping, QU Jing-qiu, YAN Jie, WU Feng, SONG De-ying. Electrochemical properties of $MmNi_{3.6}Co_{0.7}Al_{0.3}Mn_{0.4}$ alloy containing carbon nanotubes [J]. J Alloys Compd, 2003, 353: 295−300.

[6] IWAKURA C, OURA T, INOUE H, MATSUOKA M, YAMAMOTO Y. Effect of alloy composition on hydrogen diffusion in the $AB_5$-type hydrogen storage alloys [J]. J Electroanal Chem, 1995, 398(1/2): 37−41.

[7] YU X B, FENG S L, WU Z, XIA B J, XU N X. Hydrogen storage performance of Ti-V-based BCC phase alloys with various Fe content [J]. J Alloys Compd, 2005, 393: 128−134.

[8] VALØEN L O, LASIA A, JENSEN J O, TUNOLD R. The electrochemical impedance of metal hydride electrodes [J]. Electrochimica Acta, 2002, 47: 2871−2884.

[9] YUAN Xian-xia, XU Nai-xin. Determination of hydrogen diffusion coefficient in metal hydride electrode by modified Warburg impedance [J]. J Alloys Compd 2001, 329: 115−200.

[10] RAJU M, MANIMARAN K, ANANTH M V, RENGANATHAN N G. An EIS study on the capacity fades in $MmNi_{3.6}Al_{0.4}Mn_{0.3}Co_{0.7}$ metal-hydride electrodes [J]. Int J Hydrogen Energy, 2007, 32: 1721−1727.

[11] WANG Chun-sheng, SORIAGA M P, SRINIVASAN S.

Determination of reaction resistances for metal-hydride electrodes during anodic polarization [J]. J Power Sources 2000, 85: 212−223.

[12] NOTTEN P H L, HOKKELING P. Double-phase hydride forming compounds: A new class of highly electrocatalytic materials [J]. Journal of the Electrochemical Society, 1991, 138(7): 1877−1885.

[13] IWAKURA C, MATSUOKA M, ASAI K, KOHNO T. Surface modification of metal hydride negative electrodes and their charge/discharge performance [J]. J Power Sources, 1992, 38: 335−343.

[14] MATSUOKA M, ASAI K, ASAI K, FUKUMOTO K, IWAKURA C. Electrochemical characterization of surface-modified negative electrodes consisting of hydrogen storage alloys [J]. J Alloys Comp, 1993, 192: 149−151.

[15] IWAKURA C, FUKUMOTO Y, MATSUOKA M, KOHNO T, SHINMOU K. Electrochemical characterization of hydrogen storage alloys modified with metal oxides [J]. J Alloys Comp, 1993, 192: 152−154.

[16] FENG F, NORTHWOOD D O. Effect of surface modification on the performance of negative electrodes in Ni/MH batteries [J]. J Hydrogen Energy, 2004, 29: 955−960.

**(Edited by LAI Hai-hui)**